

TOWARDS PROPER SUBGRID-SCALE MODEL FOR JET AERODYNAMICS AND AEROACOUSTICS

ALEXEY P. DUBEN¹, JESUS RUANO², F. XAVIER TRIAS² AND
ANDREY V. GOROBETS¹

¹ Keldysh Institute of Applied Mathematics of Russian Academy of Sciences
4, Miusskaya Sq., Moscow, 125047, Russia
e-mail: aduben@keldysh.ru, andrey.gorobets@gmail.com

² Heat and Mass Transfer Technological Center
Technical University of Catalonia
c/Colom 11, 08222 Terrassa (Barcelona).
e-mail: jesus.ruano@upc.edu, francesc.xavier.trias@upc.edu

Key words: LES, Hybrid RANS-LES, Subgrid-scale models, Grey area mitigation, Jet

Abstract. This article presents the investigation of different grey-area mitigation (GAM) techniques towards achieving accurate subsonic turbulent round jet aerodynamics and aeroacoustics results. Combinations of new adapting subgrid length scales with 2D detecting LES models are used as the GAM technique. The numerical simulations are carried out on a set of refining meshes using two different scale-resolving codes: NOISEtte and OpenFOAM. The results show that all the considered techniques provide appropriate accuracy to predict the noise generated and the importance of both the numerical scheme and how subgrid eddy viscosity is modelled.

1 INTRODUCTION

Computational AeroAcoustics (CAA) requires high fidelity numerical solutions in the hydrodynamic region as these will be used by the acoustic solver. If hydrodynamic fields, namely velocity and pressure, are not well resolved, neither will the generated noise. A numerical simulation is composed of several selections. For example, we have to choose which discretisation of the differential operator will be used or how turbulence will be modelled; these choices will ultimately affect the quality of the results.

Regarding the numerical discretisation, as very accurate solutions are required for CAA, high-order schemes are in great demand. Among others, Shur et al. [1, 2] and Bogey [3] used high-order schemes on structured meshes. However, this kind of schemes are not always feasible. Their implementation on unstructured meshes is more computationally expensive, and using structured meshes is not always possible when dealing with industrial problems with more complex geometries. On the other hand, general second-order schemes offer a reduced computational cost in comparison with high-order schemes. Their use, however, must be accompanied by finer meshes. Tyacke et al.[4] and Fuchs et al. [5] used second-order schemes and successfully simulated a jet obtaining good jet plume hydrodynamic and acoustic results.

Finally, there is a third option consisting in using second-order schemes but with extended stencils. Such kinds of schemes allow an improvement in the quality of the results without excessively compromising the computational cost of the simulation. Bres et al. [6, 7] and Duben and Kozubskaya [8] used this type of scheme obtaining very accurate numerical solutions of both jet plume hydrodynamics and far-field noise.

Along with the numerical discretisation, how turbulence is modelled is also a critical parameter affecting the results' validity. Aiming at a good compromise between computational cost and solution accuracy, Hybrid RANS-LES Methods (HRLM) are a common choice. HRLM allow simulating relatively high Reynolds problems without requiring exaggerated fine meshes or excessively near-walls refinements. Among these methods and inside the non-zonal approaches, the Detached Eddy Simulation (DES) is one of the most used options, which has been extensively validated since its beginning and still actively developing. Regarding DES current investigations in shear-layer flows, the delay of the RANS-to-LES transition is under study. This problem, also known as the grey-area problem, is the delay of the transition from steady RANS to the time-dependent part of the mesh working on the LES regime. This transition can be triggered by reducing the subgrid eddy viscosity, ν_t . If we follow the usual definition of ν_t :

$$\nu_t = (C_{\text{LES}}\Delta_{\text{SGS}})^2 \cdot \mathcal{D}_{\text{LES}}(\bar{u}), \quad (1)$$

where Δ_{SGS} is the subgrid length scale, \mathcal{D}_{LES} is the LES model differential operator, \bar{u} is the filtered velocity, and C_{LES} is the LES constant; is easy to see that by decreasing Δ_{SGS} or \mathcal{D}_{LES} , the resulting viscosity will be smaller.

Regarding Δ_{SGS} , some advanced length scales, sensitive to the local flow, have been developed in the recent years such as Δ_ω [9, 10], $\hat{\Delta}_\omega$ [11], Δ_{SLA} [12] or Δ_{lsq} [13]. And concerning LES models, new models sensitive to two-dimensional flow patterns are the alternative to the Smagorinsky model. Among others, σ or WALE [14], or S3PQR [15] can replace it.

The here presented work is dedicated to investigating the effect of different GAM approaches in the aerodynamic and acoustic results of a subsonic round jet at $M_{\text{jet}}=0.9$. As far-field acoustics is very sensitive to the accuracy of the solution, subgrid eddy viscosity distribution should be such that it does not allow the generation of spurious noise and, at the same time, does not delay the transition from RANS to LES regime.

2 CASE FORMULATION

An immersed jet outgoing from a conical nozzle at $Re_D = 1.1 \cdot 10^6$ and $M_{\text{jet}} = 0.9$ based on jet diameter $D=0.06223$ m and velocity $U=283.7$ m/s is considered.

The computational domain, as well as both mesh and boundary conditions, are extracted from the previous work by Shur et al. [16]. The same case and data have been used a posteriori by Shur et al. [2], Duben and Kozubskaya [8], and in Pont-Vílchez et al. [17]. In these works, as well as in the here presented, the jet simulation follows a two-stage approach: first, a RANS simulation is performed, considering both inside the nozzle and the jet plume; second, only the jet plume is simulated by imposing the RANS solution as the nozzle outlet. Nonetheless, only the second stage is performed on the current work as the first stage results were kindly provided by M.Shur and M.Strelets from Peter the Great St. Petersburg Polytechnic University.

A set of 3 refining hexahedral meshes from Shur et al. [16] is used to check results convergence towards reference data. We have summarized the main parameters of these meshes in Table 1.

Table 1: Meshes parameters: total number of nodes, N_n ; number of nodes in the azimuthal direction, N_φ ; mesh sizes in the downstream, Δ_x , radial, Δ_r , and azimuthal, $r\Delta_\varphi$, directions relative to the nozzle diameter.

Parameter	Coarse	Medium	Fine
N_n	1.52M	4.13M	8.87M
N_φ	64	80	160
Δ_x/D at the nozzle exit	0.011	0.008	0.008
$\min(\Delta_r/D)$ in the shear layer	0.003	0.0025	0.0025
$r\Delta_\varphi/D$ in the shear layer	0.05	0.04	0.02

Besides the volumetric meshes, simulations require an additional set of surface meshes. These meshes are used to accumulate data, i.e. velocity and pressure, which will be used to compute acoustic sources. Details on the location of these grids will be discussed below.

3 NUMERICAL ALGORITHMS

One of the critical selections when doing a numerical simulation is which discretisation scheme is used. For this reason, two codes with considerably different numerical schemes have been used to compare the results among them.

The first code is the NOISEtte in-house research code [18, 19]. The NOISEtte is based on quasi-1D vertex-centred Edge-Based Reconstruction (EBR) [20]. The convective term uses a blending of central-difference and upwind schemes [8] with the special hybridising function extracted from Guseva et al. [21]. Noise is computed by using the FWH method [22] and using Farassat 1A formulation [23] which uses the retarded time concept.

The second code is the OpenFOAM software. The OpenFOAM code is based on a collocated unstructured finite-volume approach. The convective term consists of a hybrid scheme which blends between a 2nd order central-difference scheme and a 2nd order upwind scheme [24]. Noise in OpenFOAM simulations is also computed with the FWH method [22]. However, it uses an in-house code based on Fourier Transformation, which converts the temporal source signals into spectral ones. This method avoids retarded times as the phase shift between source and observer is computed.

Acoustic sources are stored and accumulated at the set of non-overlapping surface meshes, whose location can be seen marked with yellow lines in Figure 1. Source contribution to the total amount of noise is averaged on both the conical sleeve surfaces and the outflow discs [1, 25] to reduce significantly spurious noise. Additionally, for each observer angle position, noise is computed at 32 equidistant azimuthally distributed points and then averaged to improve results convergence.

Data is stored at integration surfaces at least for $250D/U_{\text{jet}}$ in order to ensure a better convergence of the low-frequency range of the acoustic spectrum. The initial transient period to avoid initial condition effects lasts for about another $250D/U_{\text{jet}}$. However, this period could be greatly reduced by using either an evolved flow from another GAM approach in the same mesh or by interpolating an evolved flow from another mesh, being it coarser or finer.

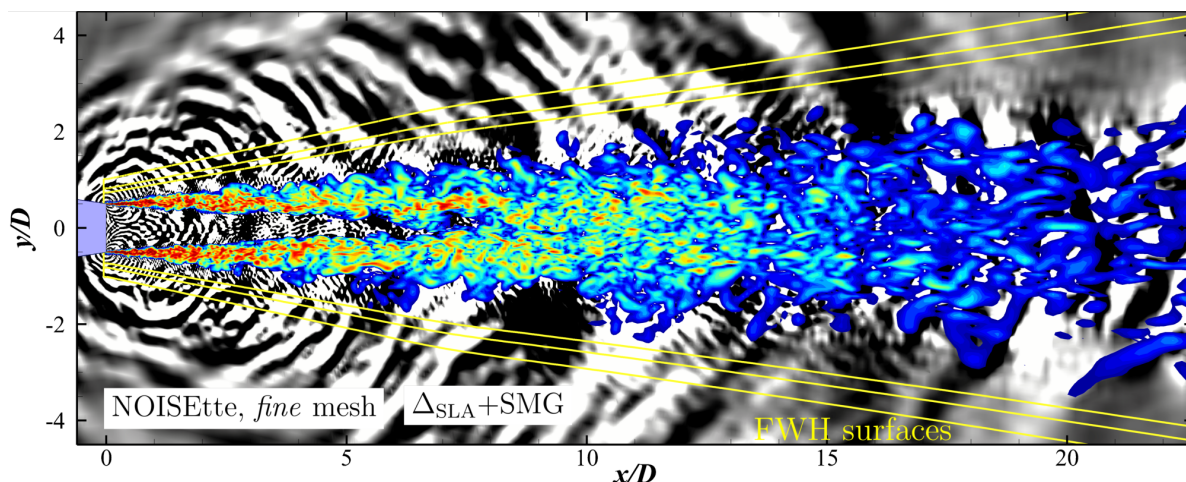


Figure 1: The instantaneous flow field in the jet plume region (the NOISEtte simulation on the finest mesh using the $\Delta_{\text{SLA}}+\text{SMG}$ approach). The yellow lines mark the location of the FWH control surfaces

4 RESULTS AND DISCUSSION

In this section, the numerical results will be commented and compared with empirical data. Jet-plume aerodynamics, i.e. time-averaged streamwise velocity and its fluctuations, are evaluated using reference data from similar jets from Lau et al. [26, 27], Simonich et al. [28], Arakeri et al. [29] and Bridges and Wernet [30]. Reference experimental data regarding far-field values, i.e. Overall Sound Pressure Level (OASPL) and 1/3 octave spectra, are extracted from Viswanathan experiments [31].

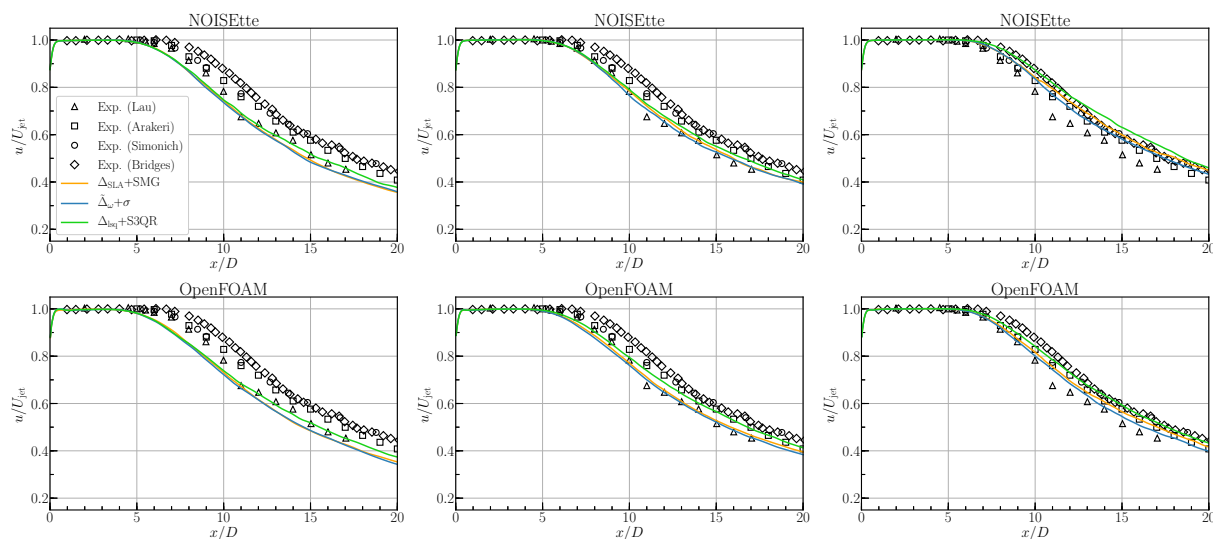


Figure 2: Centerline distributions of the streamwise velocity obtained using NOISEtte (top) and OpenFOAM (bottom) on a set of refining meshes (from left to right).

4.1 Hydrodynamic results

The time-averaged results of both velocity and its RMS values in the jet centerline are shown in Figures 2 and 3. Independently of the used code, mesh refinement leads to better numerical results as those get closer to the experiment. Analysing them in more detail, it can be stated that NOISEtte has better results as these are closer to the experimental values thanks to the higher-accuracy schemes used. Averaged velocity distributions in OpenFOAM always show a slightly lesser potential core length than NOISEtte when the same meshes are compared. Nonetheless, OpenFOAM results are still in very good agreement with the experiment.

Both codes show good convergence rates regarding velocity fluctuations as numerical results get closer to the reference data as the mesh is refined. It should be noticed that for values of $x/D > 10$, the experimental results seem to bifurcate as two different trends appear. However, numerical results in the three meshes and in both used codes are always kept between the region that these two trends conform. Again, the higher-accuracy schemes used by NOISEtte lead to slightly more accurate results than those produced by OpenFOAM. Nevertheless, the results obtained with OpenFOAM can still be considered good and very close to the reference data. Analysing results in the coarsest and the medium meshes, NOISEtte does not show any noticeable differences between the selected GAM approaches. However, OpenFOAM has two slightly different trends near the peak value: $\Delta_{\text{lsq}}+\text{S3QR}$ behaves differently than the other two approaches. This is explained by the fact that in the centerline for values higher than $x/D \sim 5$, Δ_{lsq} trends to Δ_{vol} while the other two options trend to Δ_{max} . Therefore, there are differences in the amount of turbulent eddy viscosity added that explain the strength of the oscillations, i.e. higher oscillations amplitude at higher diffusivity values. This difference is still present in the finest grid, but its effects are more attenuated.

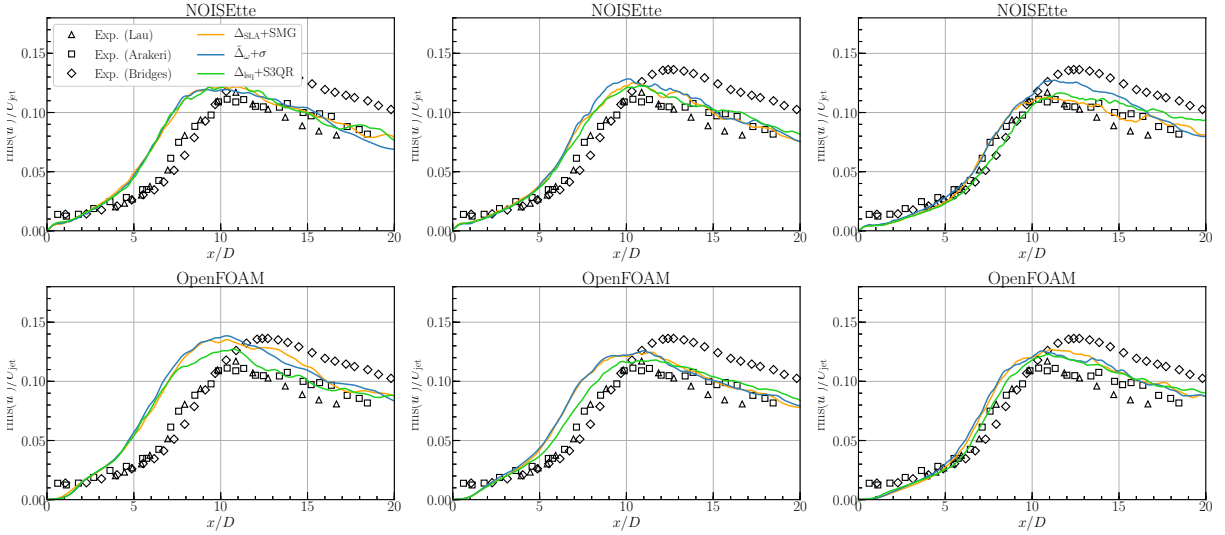


Figure 3: Centerline distributions of the streamwise velocity pulsations RMS obtained using NOISEtte (top) and OpenFOAM (bottom) on a set of refining meshes (from left to right).

4.2 Acoustic results

In contrast to the jet near field hydrodynamics, where both codes show very similar results, the obtained acoustics are very different.

The Overall Sound Pressure Level (OASPL) is presented in Figure 5. As can be seen, NOISEtte exhibits a very good convergence for observers at all angles, defining their position as shown in Figure 4. Refining the mesh leads to obtaining better numerical results. However, it can be noticed that for very high angles and only at the most refined mesh, the $\Delta_{lsq} + S3QR$ approach underestimates OASPL. Nonetheless, it should be said that such kind of angles should not be considered to evaluate the validity of a model.

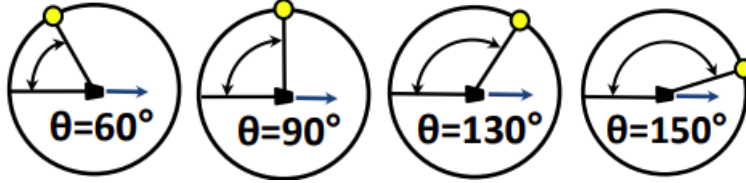


Figure 4: Angles position for 60, 90, 130 and 150°. Blue arrow indicates downstream direction.

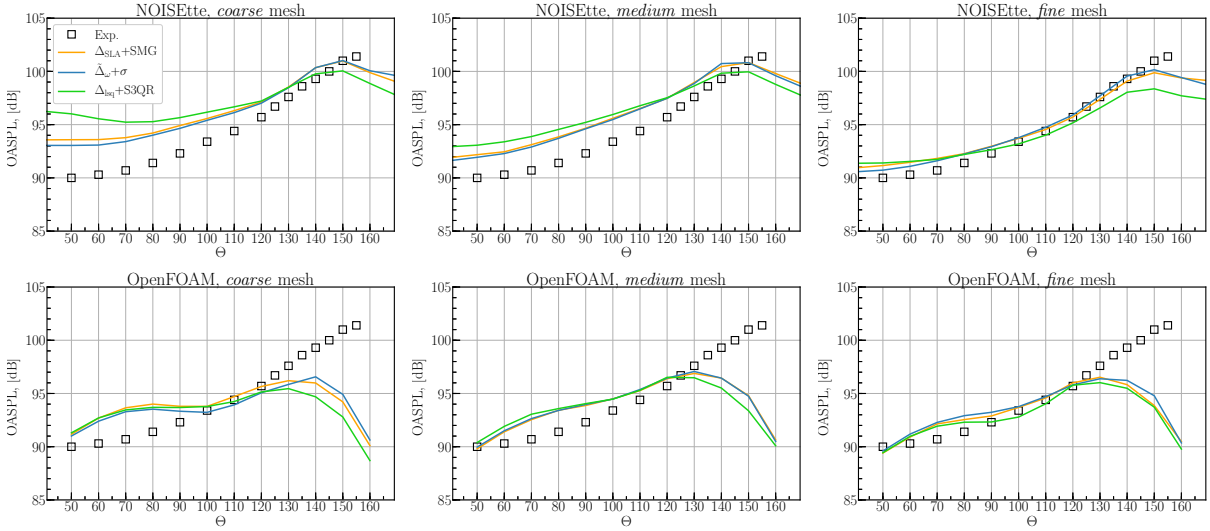


Figure 5: Overall Sound Pressure Level directivity obtained using NOISEtte (top) and OpenFOAM (bottom) on a set of refining meshes (from left to right).

OpenFOAM, on the other hand, exhibits a totally different behaviour. OASPL at low angles ($< 120^\circ$) is reasonably well computed at all meshes, obtaining better results as the mesh is refined. However, OASPL at higher angles is highly underestimated.

Noise at such angles is generated by the big vortices going downstream of the domain. As the shape of these vortices is not well kept by the general 2nd-order schemes used in OpenFOAM, i.e. they are more dissipative and dispersive, this leads to a wrong production noise mechanism. Consequently, this produces an error in OASPL quantification in such angles.

Moreover, the effect of a specific GAM technique in comparison with another becomes harder to distinguish when general 2nd-order schemes are used. This occurs because the amount of artificial diffusion that the numerical scheme adds is higher when using such schemes. Consequently, this makes it harder to distinguish between GAM and scheme contributions. In contrast, the small amount added by the high-accuracy schemes allows distinguishing the differences between GAM approaches more easily in the OASPL results.

Regarding the high OASPL values at low angles obtained by the NOISEtte code, the 1/3 octave spectra in Figure 6 can be used to find an explanation. In the coarse mesh, NOISEtte exhibits a zone with results higher than the experiment for $St \sim 1$. This is related to the generation of spurious noise at the beginning of the shear-layer region due to the nonphysical RANS-to-LES transition in conjunction with the low inherent diffusivity of the numerical scheme that leads to the generation of instabilities. As can be seen, this overestimation in the results gets more attenuated for finer meshes.

In contrast, OpenFOAM results show a less pronounced results overestimation that, again, is attenuated as the mesh is refined. Moreover, it can be seen that OpenFOAM results drop earlier than the NOISEtte ones; the high frequencies start to be underestimated first by OpenFOAM than by NOISEtte. This causes that using OpenFOAM, on average, the overestimation in low frequencies is compensated by an underestimation in the high ones in the low-angle region.

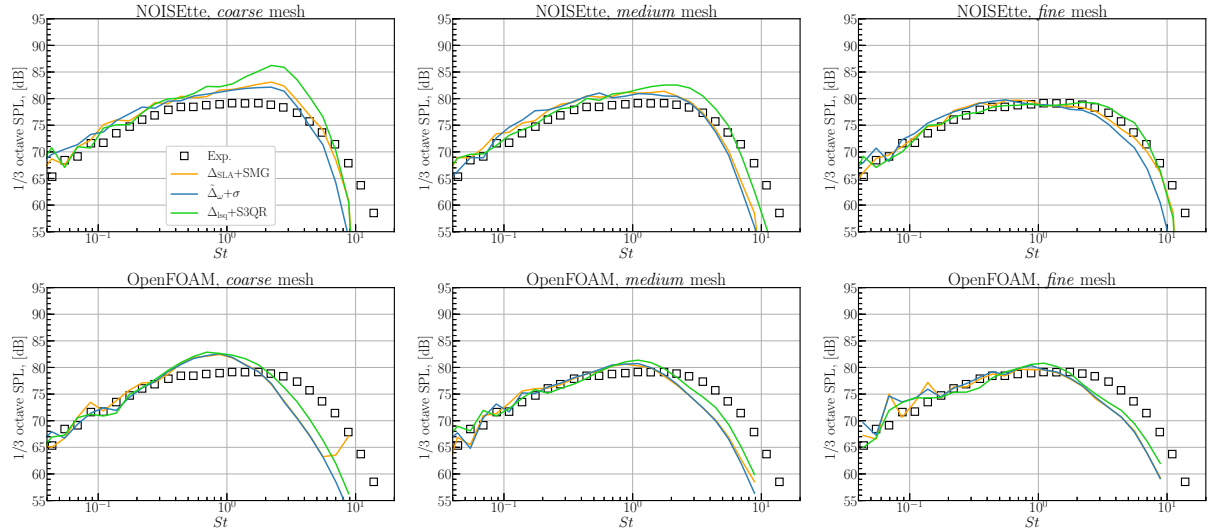


Figure 6: 1/3rd-octave integrated spectrums at the observer angle $\theta = 60^\circ$.

Once low-angles have been commented on, the higher ones should be studied too. Analysing 1/3 octave spectra in Figure 7 can help to understand why the computed noise in these angles does or does not match the experimental results.

NOISEtte results using the coarse and medium meshes almost perfectly match between numerical and experimental OASPL. Therefore, results on Figure 7 are expected. There is not a noticeable mismatch between numerical 1/3 octave spectrums and the reference data. However, on the finest mesh, there is a slight underestimation of the OASPL. 1/3 octave spectrum of this mesh shows an underestimation in the range $0.2 < St < 0.9$ for all the selected GAM approaches, being more noticeable for the $\Delta_{\text{lsq}}+\text{S3QR}$ approach. However, and as was previously said, such angles are not decisive in evaluating the validity or not of the GAM.

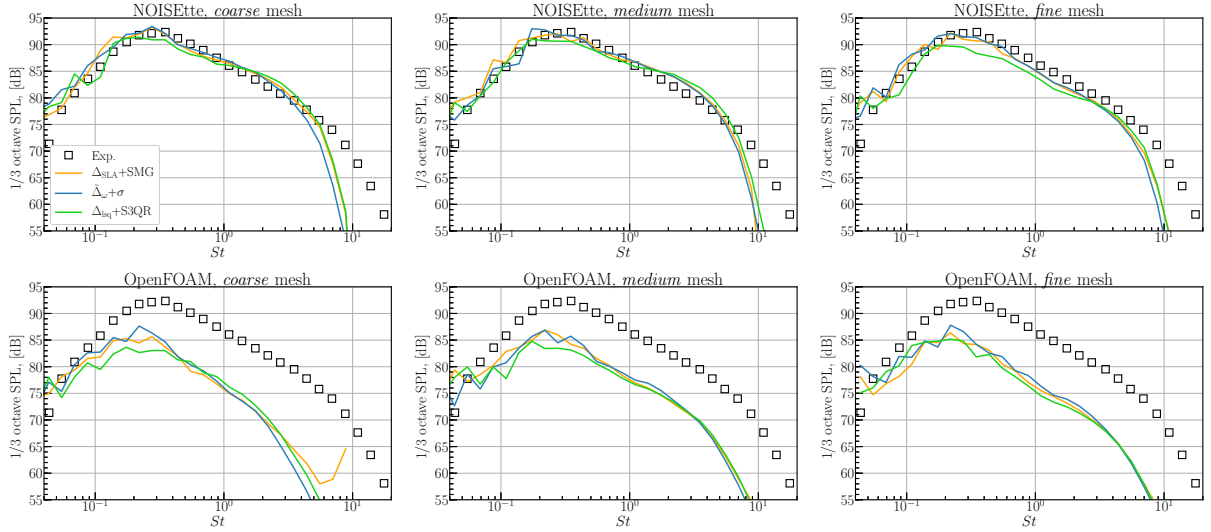


Figure 7: 1/3rd-octave integrated spectrums at the observer angle $\theta = 150^\circ$.

As has been previously commented, there is a very strong underestimation of the noise levels at high observer angles when OpenFOAM is used. The noise generation mechanism explains this at such kinds of angles. Vortices travelling far downstream the nozzle are responsible for generating noise at very high angles. Therefore, they should be correctly simulated during the whole domain until they reach the outflow discs. OpenFOAM uses a blend of dissipative and non-dissipative 2nd order schemes, which, due to the highly dispersive and dissipative nature [32], is not able to provide proper evolution of turbulent structures. In consequence, vortices arriving at the outflow discs are more dissipated and with a more distorted shape than when high-accuracy schemes are employed.

5 CONCLUSIONS

The numerical results of an immersed subsonic round jet using two different schemes on a set of refining meshes have been presented. It can be concluded that GAM techniques are critical at achieving good hydrodynamic and acoustic results when simulating it. In this work, only three different approaches have been considered; in previous work, those approaches with non-acceptable hydrodynamic results were discarded.

The obtained hydrodynamic results show that high-accuracy schemes are always better than if general 2nd order ones are used. Nonetheless, both have shown very accurate results of averaged centerline velocity and its fluctuations. The three GAM techniques selected have shown very similar behaviour. The minor differences between them are explained by how Δ behaves in the fully turbulent developed region: Δ_{lsq} trends to Δ_{vol} while both Δ_{SLA} and $\tilde{\Delta}_{\omega}$ trend to Δ_{max} . The turbulence model, assuming one sensitive to two-dimensional flow pattern is used or Δ_{SLA} is used, has been found to have a minimal impact on the numerical results.

On the other hand, acoustics results present remarkable differences when different schemes were used. NOISEtte has shown very good convergence properties in both OASPL and 1/3 octave spectra. The overestimation at the lower observer angles is explained by the generation of spurious noise due to the RANS-to-LES transition in the initial part of the shear layer that cannot be attenuated by the low-dissipative used schemes. On the other hand, the highest observer angles are well computed in all the three selected meshes and with all the three GAM approaches, with a slight underestimation of the OASPL when the combination $\Delta_{\text{lsq}}+\text{S3QR}$ is used. In contrast, OpenFOAM has shown good accuracy at low observer angles. This is explained by a less pronounced overestimation due to the RANS-to-LES transition in conjunction with a faster decay at the highest frequencies. Overall, this leads to an equilibrium between slightly overestimated frequencies with slightly underestimated ones. Nonetheless, noise at the highest observer angles is not well reproduced due to the highly dispersive and diffusive nature of the used numerical schemes, which are not able to keep vortices' shape travelling downstream the nozzle.

Acknowledgements

The work of J.R.P. and F.X.T. has been financially supported by the project RETOtwIn (PDC2021-120970-I00) funded by MCIN/AEI/10.13039/501100011033 and European Union Next Generation EU/PRTR. J.R.P. is supported by a *FI-DGR 2015* predoctoral contract financed by *Generalitat de Catalunya*, Spain.

REFERENCES

- [1] M. L. Shur, P. R. Spalart, and M. K. Strelets, “Noise prediction for increasingly complex jets. part I: Methods and tests,” *International Journal of Aeroacoustics*, vol. 4, pp. 213–245, jul 2005.
- [2] M. L. Shur, P. R. Spalart, and M. K. Strelets, “Jet noise computation based on enhanced DES formulations accelerating the RANS-to-LES transition in free shear layers,” *International Journal of Aeroacoustics*, vol. 15, pp. 595–613, jul 2016.
- [3] C. Bogey, “Grid sensitivity of flow field and noise of high-reynolds-number jets computed by large-eddy simulation,” *International Journal of Aeroacoustics*, vol. 17, pp. 399–424, may 2018.
- [4] J. Tyacke, I. Naqavi, Z.-N. Wang, P. Tucker, and P. Boehning, “Predictive large eddy simulation for jet aeroacoustics—current approach and industrial application,” *Journal of Turbomachinery*, vol. 139, mar 2017.
- [5] M. Fuchs, C. Mockett, M. Shur, M. Strelets, and J. C. Kok, “Single-stream round jet at $M = 0.9$,” in *Notes on Numerical Fluid Mechanics and Multidisciplinary Design*, pp. 125–137, Springer International Publishing, jul 2017.
- [6] G. A. Brès, F. E. Ham, J. W. Nichols, and S. K. Lele, “Unstructured large-eddy simulations of supersonic jets,” *AIAA Journal*, vol. 55, pp. 1164–1184, apr 2017.
- [7] G. A. Brès, P. Jordan, V. Jaunet, M. L. Rallic, A. V. G. Cavalieri, A. Towne, S. K. Lele, T. Colonius, and O. T. Schmidt, “Importance of the nozzle-exit boundary-layer state in subsonic turbulent jets,” *Journal of Fluid Mechanics*, vol. 851, pp. 83–124, jul 2018.
- [8] A. P. Duben and T. K. Kozubskaya, “Evaluation of quasi-one-dimensional unstructured method for jet noise prediction,” *AIAA Journal*, vol. 57, pp. 5142–5155, dec 2019.
- [9] N. Chauvet, S. Deck, and L. Jacquin, “Zonal detached eddy simulation of a controlled propulsive jet,” *AIAA Journal*, vol. 45, pp. 2458–2473, oct 2007.
- [10] S. Deck, “Recent improvements in the zonal detached eddy simulation (ZDES) formulation,” *Theoretical and Computational Fluid Dynamics*, vol. 26, pp. 523–550, oct 2011.
- [11] C. Mockett, M. Fuchs, A. Garbaruk, M. Shur, P. Spalart, M. Strelets, F. Thiele, and A. Travin, “Two non-zonal approaches to accelerate RANS to LES transition of free shear layers in DES,” in *Progress in Hybrid RANS-LES Modelling*, pp. 187–201, Springer International Publishing, 2015.
- [12] M. L. Shur, P. R. Spalart, M. K. Strelets, and A. K. Travin, “An enhanced version of DES with rapid transition from RANS to LES in separated flows,” *Flow, Turbulence and Combustion volume*, vol. 95, pp. 709–737, jun 2015.
- [13] F. X. Trias, A. Gorobets, M. H. Silvis, R. W. C. P. Verstappen, and A. Oliva, “A new subgrid characteristic length for turbulence simulations on anisotropic grids,” *Physics of Fluids*, vol. 29, p. 115109, nov 2017.

- [14] F. Nicoud, H. B. Toda, O. Cabrit, S. Bose, and J. Lee, “Using singular values to build a subgrid-scale model for large eddy simulations,” *Physics of Fluids*, vol. 23, p. 085106, aug 2011.
- [15] F. X. Trias, D. Folch, A. Gorobets, and A. Oliva, “Building proper invariants for eddy-viscosity subgrid-scale models,” *Physics of Fluids*, vol. 27, p. 065103, jun 2015.
- [16] M. Shur, P. Spalart, and M. Strelets, “LES-based evaluation of a microjet noise reduction concept in static and flight conditions,” *Procedia Engineering*, vol. 6, pp. 44–53, 2010.
- [17] A. Pont-Vílchez, A. Duben, A. Gorobets, A. Revell, A. Oliva, and F. X. Trias, “New strategies for mitigating the gray area in delayed-detached eddy simulation models,” *AIAA Journal*, vol. 59, pp. 3331–3345, sep 2021.
- [18] A. Gorobets, “Parallel algorithm of the NOISEtte code for CFD and CAA simulations,” *Lobachevskii Journal of Mathematics*, vol. 39, pp. 524–532, may 2018.
- [19] A. Gorobets and P. Bakhvalov, “Heterogeneous CPU+GPU parallelization for high-accuracy scale-resolving simulations of compressible turbulent flows on hybrid supercomputers,” *Computer Physics Communications*, vol. 271, p. 108231, feb 2022.
- [20] I. Abalakin, P. Bakhvalov, and T. Kozubskaya, “Edge-based reconstruction schemes for unstructured tetrahedral meshes,” *International Journal for Numerical Methods in Fluids*, vol. 81, pp. 331–356, dec 2015.
- [21] E. K. Guseva, A. V. Garbaruk, and M. K. Strelets, “An automatic hybrid numerical scheme for global RANS-LES approaches,” *Journal of Physics: Conference Series*, vol. 929, p. 012099, nov 2017.
- [22] “Sound generation by turbulence and surfaces in arbitrary motion,” *Philosophical Transactions of the Royal Society of London. Series A, Mathematical and Physical Sciences*, vol. 264, pp. 321–342, may 1969.
- [23] F. Farassat, “Linear acoustic formulas for calculation of rotating blade noise,” *AIAA Journal*, vol. 19, pp. 1122–1130, sep 1981.
- [24] A. Travin, M. Shur, M. Strelets, and P. R. Spalart, “Physical and numerical upgrades in the detached-eddy simulation of complex turbulent flows,” in *Fluid Mechanics and Its Applications*, pp. 239–254, Springer Netherlands, 2002.
- [25] P. R. Spalart and M. L. Shur, “Variants of the flowcs williams - hawkings equation and their coupling with simulations of hot jets,” *International Journal of Aeroacoustics*, vol. 8, pp. 477–491, jul 2009.
- [26] J. C. Lau, P. J. Morris, and M. J. Fisher, “Measurements in subsonic and supersonic free jets using a laser velocimeter,” *Journal of Fluid Mechanics*, vol. 93, pp. 1–27, jul 1979.
- [27] J. C. Lau, “Effects of exit mach number and temperature on mean-flow and turbulence characteristics in round jets,” *Journal of Fluid Mechanics*, vol. 105, p. 193, apr 1981.

- [28] J. Simonich, S. Narayanan, T. Barber, and M. Nishimura, “High subsonic jet experiments. i - aeroacoustic characterization, noise reduction and dimensional scaling effects,” in *6th Aeroacoustics Conference and Exhibit*, American Institute of Aeronautics and Astronautics, jun 2000.
- [29] V. H. Arakeri, A. Krothapalli, V. Siddavaram, M. B. Alkisar, and L. M. Lourenco, “On the use of microjets to suppress turbulence in a mach 0.9 axisymmetric jet,” *Journal of Fluid Mechanics*, vol. 490, pp. 75–98, sep 2003.
- [30] J. Bridges and M. Wernet, “Establishing consensus turbulence statistics for hot subsonic jets,” in *16th AIAA/CEAS Aeroacoustics Conference*, American Institute of Aeronautics and Astronautics, jun 2010.
- [31] K. Viswanathan, “Aeroacoustics of hot jets,” *Journal of Fluid Mechanics*, vol. 516, pp. 39–82, oct 2004.
- [32] J. Ruano, A. B. Vidal, J. Rigola, and F. X. Trias, “A new general method to compute dispersion errors on cartesian stretched meshes for both linear and non-linear operators,” *Computer Physics Communications*, vol. 271, p. 108192, 2022.